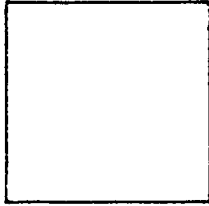


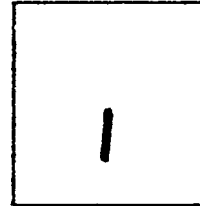
PHOTOGRAPH THIS SHEET

1951780

DTIC ACCESSION NUMBER



LEVEL



INVENTORY

WALTER 397.6/1

DOCUMENT IDENTIFICATION

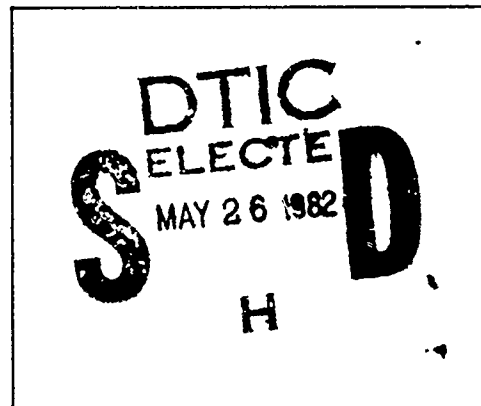
**DISTRIBUTION STATEMENT A**  
Approved for public release;  
Distribution Unlimited

JUN 1960

DISTRIBUTION STATEMENT

ACCESSION FOR	
NTIS	GRA&I <input checked="" type="checkbox"/>
DTIC	TAB <input type="checkbox"/>
UNANNOUNCED	<input type="checkbox"/>
JUSTIFICATION	
BY	
DISTRIBUTION /	
AVAILABILITY CODES	
DIST	AVAIL AND/OR SPECIAL
A	

DTIC  
COPY  
INSPECTED  
Z



DATE ACCESSIONED

DISTRIBUTION STAMP

**UNANNOUNCED**

82 05 25 115

DATE RECEIVED IN DTIC

PHOTOGRAPH THIS SHEET AND RETURN TO DTIC-DDA-2

AD

# /  
WAL TR 397.6/1



# WATERTOWN ARSENAL LABORATORIES

PLASTIC ROTATING BANDS: EVALUATION OF TWO PLASTICS

TECHNICAL REPORT NO. WAL TR 397.6/1

BY

K. D. ROBERTSON

JUNE 1960

O.O. PROJECT: TW-120, IMPROVEMENT OF  
ARTILLERY AMMUNITION

D/A PROJECT: 5A04-03-006

WATERTOWN ARSENAL  
WATERTOWN 72, MASS.

OFFICIAL FILE COPY

AD A551780

AD

Plastics  
Rotating band  
materials

PLASTIC ROTATING BANDS: EVALUATION OF TWO PLASTICS

Technical Report No. WAL TR 397.6/1

By  
K. D. Robertson

June 1960

O.O. Project: TW-120, Improvement of  
Artillery Ammunition  
D/A Project: 5A04-03-006

Not for distribution to NATO Governments.

WATERTOWN ARSENAL  
WATERTOWN 72, MASS.


WATERTOWN ARSENAL LABORATORIES

TITLE

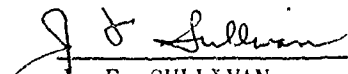
PLASTIC ROTATING BANDS: EVALUATION OF TWO PLASTICS

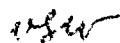
ABSTRACT

A method is described to determine the maximum allowable driving edge pressure on rotating band materials. This method is then applied to determine the maximum allowable driving edge pressure for two plastic materials, Nylon (Zytel 101) and Boltaron (6200). An error analysis of the apparent driving edge pressure is included. Upper and lower limits on the experimentally determined maximum allowable driving edge pressure are given. The values of the maximum allowable driving edge pressures for Nylon and Boltaron are 20,000 and 16,750 psi respectively.

  
KENNETH D. ROBERTSON  
Engineer

APPROVED:

  
J. F. SULLIVAN  
Director  
Watertown Arsenal Laboratories

REPORT APPROVED  
Date- 15<sup>th</sup> 2 68  
WAL Board of Review  
Chairman- 

## PURPOSE AND SCOPE

The purpose of this investigation was to determine the maximum allowable driving edge pressure of Nylon and Bortaron rotating bands.

## INTRODUCTION

Until recently almost all rotating bands were made from gilding metal, and proved very satisfactory. During emergencies, however, this material is in great demand for many purposes, and therefore a substitute material is desired. Plastics have been investigated as a possible substitute material,<sup>1</sup> and some appear promising. The properties of these new materials must now be evaluated.

One of the properties of interest to the designer is the maximum allowable driving edge pressure. This property is a function of the material, the geometry of the gun tube rifling, and the conditions of loading. It is generally considered to be that pressure which will cause no measurable displacement of the driving edge. This displacement may occur as a result of wear or as a result of elastic or plastic deformation of the band.

The maximum allowable driving edge pressure is often determined by a firing test. In a test of this nature, all the factors influencing this pressure are present. The projectiles are recovered, the driving edge displacement measured and the driving edge pressure is computed from formulas. In the present test, a different procedure was employed. The maximum driving edge pressure in this case was determined from static tests. In this manner, the strain rate effect and the effects of wear were eliminated. These effects can be considered separately, and used to modify the results of this investigation.

## NOMENCLATURE

- D - Average bore diameter
- $D_g$  - Gun tube groove diameter
- $D_\ell$  - Gun tube land diameter
- E - Elastic Modulus
- $F_a$  - Axial force on push rod
- $\ell$  - Band length
- N - Number of lands
- $P_b$  - Radial band pressure

<sup>1</sup>COHN, GUNTHER, A Survey of Plastics for Rotating Bands (U), The Franklin Institute Laboratories for Research and Development, Contract DA-36-034-ORD-1215-RD, WAL No. 780/452-19(c), 30 April 1954.

$P_i$  - Internal radial pressure  
 $T_a$  - Applied torque  
 $Z$  - Ratio of axial distance to bore radius  
 $\delta_{de}$  - Driving edge displacement  
 $\epsilon_\theta$  - Gun tube tangential strains  
 $\phi$  - Angle of rifling with axis of gun tube  
 $\mu$  - Coefficient of sliding friction  
 $\sigma_{de}$  - Driving edge pressure

### TEST EQUIPMENT

The dismantled test setup is shown in Figure 1. It consists of a standard 37mm gun tube section, modified as shown in Figure 2; a push rod, shown in detail in Figure 3; a torque collar, shown in detail in Figure 4; and an adjustable collar, shown in Figure 5.

The gun tube section was modified for purposes of this investigation. The rifling was removed for the first five inches to allow assembly of the gun tube, torque collar, push rod, and rotating band. A new forcing cone was machined at the end of this five-inch section. This was followed by a 2.4-inch length of standard rifling shown in Figure 6. Beyond this point, the rifling was removed to allow free passage of the band for removal at the muzzle end.

The torque collar shown in Figure 4 fitted over the push rod and into the slotted breech end of the gun tube. The internal splines of the torque collar engaged longitudinal grooves in the push rod, while the external fins engaged slots in the gun tube. When the torque collar was engaged, no relative rotation between the gun tube and push rod was possible at the torque collar. Opposing torques developed at the driving edge and transmitted through the gun tube and push rod were thus cancelled at the torque collar.

The adjustable collar (Figure 5) was used to disengage the torque collar at the end of a test, and thus release the torque on the band.

The push rod was grooved longitudinally to slide in the torque collar. The diameter at one section of the push rod was reduced to accommodate strain gages used to determine torque. The lower end of the push rod was splined to prevent the band from turning on the push rod.

### INSTRUMENTATION

SR-4 strain rosettes, Type AR-1, were mounted on the push rod as shown in Figure 3 to determine torque. Strain rosettes, Type AX-5, were mounted on the tube, as shown in Figure 2, to determine band pressure.

The shaft was initially calibrated in a torque machine, and the resulting calibration curve is shown in Figure 7. The torque gages were connected in a four-arm bridge, as shown in Figure 3, and were self-compensating for axial and bending strains.

The strains were read on SR-4 strain indicators, which were calibrated in 10 micro-inch increments.

### TEST PROCEDURE

A band was mounted on the push rod and inserted into the breech end of the gun tube. The push rod was rotated until the torque collar was engaged. The torque collar was then raised, and the band was forced into the rifling until engraving was complete. At this time, the torque collar was lowered into the engaging position, and the torque reading strain indicator zeroed. The band was then pushed further into the tube until the desired torque strain reading was developed. The torque collar was then disengaged to remove the torque and the band was pushed through the tube. The axial load and maximum tangential strain were read simultaneously as the band passed under the gages on the tube. The band was removed from the tube at the muzzle end.

Fifteen Boltaron (6200) and fifteen Nylon (Zytel 101) bands were tested, as described above. In general, three bands were tested at each of several driving edge pressures. The results of these tests are listed in Tables I and II.

### GENERAL CONSIDERATIONS

#### Driving Edge Displacement

The groove of a rotating band is formed in the forcing cone of a gun tube by the rifling which acts as a die. The band is plastically deformed by the rifling and forced to conform to the rifling geometry during engraving. A pressure, and consequently a strain, is developed on both walls of the groove by this engraving action. The driving edge of the band, which constitutes one of these groove walls, is further strained after engraving is completed by the inertia forces accompanying the acceleration. As the driving edge is further strained by these inertia forces, the opposite groove wall experiences a reduction in strain and consequently recovers elastically. The geometry of the driving edge conforms to the rifling geometry, at least while the driving edge stress is increasing, but on recovery, the opposite groove wall may not retain the rifling geometry. As the driving edge is unloaded after it has been strained plastically or elastically, its geometry may also change.

The permanent change in groove width caused by driving edge pressure, measured after the band has been unloaded, is generally considered to be

driving edge displacement. The magnitude of this driving edge displacement is therefore a measure of a change of dimension after the load causing this change has been removed. An accurate measure of the driving edge displacement would require the evaluation of the change in distance between two points on the band - one point on the driving edge and the other point on the opposite groove wall, both points easily identifiable before and after loading. A measurement of this type is very difficult to obtain and was not attempted in this investigation.

In this investigation, the term "Driving Edge Displacement" will mean the change in groove width due to torque, measured across the groove, after removal of torque, between the points where the groove walls become tangent to the outer periphery of the band, as shown in Figure 8.

The tangent point adjacent to the driving edge of a torqued band was not clearly identifiable with the corresponding point in the untorqued band in this investigation. Thus the measured driving edge displacements in this investigation were not true driving edge displacements. Instead, they merely represent observations of the movement at the tangency point due to applied torque. However, this observation in itself is sufficient to determine the pressure at which permanent deformation commences since a change in the position of the tangency point represents permanent deformation.

The geometry of a band changes as it is unloaded as mentioned previously. The band expands radially and circumferentially as the radial band pressure is removed and the band land expands circumferentially as the driving edge pressure is removed. Because of these changes in geometry, which can be large in materials of low modulus, the groove width of the unloaded band may differ considerably from the mating gun land width. It would be erroneous then to use the gun land width as the true undeformed band groove width. Instead, in this investigation the true undeformed band groove width was determined by tests. A rotating band was engraved and forced through the tube with no torque applied. The groove width of this band was then considered to be the undeformed groove width. All subsequent driving edge displacements were based on this minimum groove width.

After testing, the bands were mounted on a shaft and the groove widths measured by means of an optical comparator, as shown in Figure 9. The driving edge displacements were viewed from a position perpendicular to the periphery of the band. A photomicrograph of a typical observed surface magnified 20 times is shown in Figure 8.

The optical comparator was graduated in 0.001mm. Measurement of the distance between two clearly identifiable points was thus possible to an accuracy of  $\pm 0.00003937$  inch. Measurements of groove width between two reference points however, varied by as much as  $\pm 0.0015$  inch. This indicated that the reference points were not interpreted identically each time. The groove width was measured between the two points, shown in Figure 8. These points corresponded to the tangency points between the groove



wall and the outer periphery of the band. A photomicrograph of a groove profile magnified 200 times is shown in Figure 10. It will be observed that the edges of the groove are rounded. The rounding of these edges introduces some error into the measurement of groove width. When viewed from above, as in Figure 8, the change in slope of the groove walls near the point of tangency (Figure 10) appears as a line of demarcation between light and dark areas. The rate of change of slope is thus seen to be the deciding factor in determining the accuracy of measurement of the tangency point. The limits of accuracy in measuring the tangency point are  $\pm 0.0015$  inch. This would indicate that a significant change in slope must occur in 0.0015 inch of the tangency point. A photomicrograph of the groove geometry in the vicinity of the tangency point (Figure 10) shows a detectable change in slope in 0.0015 inch and explains the limits.

#### Evaluation of $\mu$

The apparent coefficient of friction,  $\mu$ , was required in order to compute the actual driving edge stress. This apparent coefficient of friction was determined experimentally for each band that had an applied driving edge pressure. In each case, the torque was reduced to zero and the axial force and band pressure determined simultaneously. The coefficient of friction was then determined from the equation developed in Appendix A.

#### Radial Band Pressure Calculation

The radial band pressure was determined by the method outlined in Reference 2 in which the ratio of outer surface strain to the internal pressure  $E\epsilon_{\theta}/P_i$  is given as a function of the ratio of axial distance to bore radius  $Z$ . The maximum value of this ratio was  $E\epsilon_{\theta}/P_i = 0.55$ . The maximum outer surface strain was determined when the band was under the gage mounted on the tube. With the value of  $\epsilon_{\theta}$  and the ratio  $E\epsilon_{\theta}/P_i$  known, the internal pressure, i.e., radial band pressure,  $P_b$  could be calculated directly.

#### Driving Edge Pressure

The driving edge pressure,  $\sigma_{de}$ , can be expressed as a function of the applied torque,  $T_a$ , the radial band pressure,  $P_b$ , the apparent coefficient of friction,  $\mu$ , and certain geometric parameters, by solving the torque equilibrium equation of the free body diagram shown in Figure 11. This functional relationship is expressed below:

$$\sigma_{de} = \frac{8T_a + \mu \pi P_b \ell (D_g + D_{\ell})^2 \sin \phi}{\ell N (D_g^2 - D_{\ell}^2) (1 - \mu \tan \phi)}$$

<sup>2</sup>RADKOWSKI, P. P., BLUHM, J. I., and BOWIE, O. L., Editors, *Thick-Walled Cylinder Handbook - Stresses and Strains in Elastic, Thick-Walled, Circular Cylinders Resulting from Axially Symmetric Loadings*, Watertown Arsenal Laboratory, W4L No. 893/172, 1 December 1954.

The torque corresponding to the measured torque strain reading was read from the calibration curve of Figure 7. This value of torque and the value of radial band pressure,  $P_b$ , plus the apparent coefficient of friction,  $\mu$ , determined as described previously, along with the known geometric parameters, were substituted into the above equation to determine the driving edge pressure,  $\sigma_{de}$ . The error in driving edge pressure as determined in Appendix B is negligible. Values of driving edge stress,  $\sigma_{de}$ , and the corresponding values of driving edge displacement,  $\delta_{de}$ , are tabulated in Tables I and II, and plotted in Figures 12 and 13.

#### Determination of the Maximum Allowable Driving Edge Pressure

The driving edge pressure,  $\sigma_{de}$ , was plotted as a function of the driving edge displacement,  $\delta_{de}$  (Figures 12 and 13). These curves were then extrapolated to zero driving edge displacement, and the corresponding pressure read from the curve. This pressure was then considered to be the maximum allowable driving edge pressure. For Nylon (Zytel 101) the maximum allowable pressure was 20,000 psi, while for Boltaron (6200) this pressure was 16,750 psi. The limits of accuracy of the maximum allowable driving edge pressure are shown by the dotted lines in Figures 12 and 13. These limits were determined by the error in measuring the driving edge displacement,  $\delta_{de}$ . The limits for Nylon are  $\pm 6,000$  psi and for Boltaron, these limits are  $\pm 4,250$  psi.

#### DISCUSSION OF RESULTS

1. The results indicate that the maximum allowable driving edge pressure under static loading conditions is 20,000 psi for Nylon (Zytel 101) and 16,750 psi for Boltaron (6200). These values may increase under dynamic loading conditions.
2. An approximate solution for the elastic displacement of the driving edge, Appendix C, indicates that for materials of low modulus, large elastic displacements are likely to occur.
3. The approximate solution of the elastic driving edge displacements (Appendix C) further indicates that the measurement of permanent driving edge displacement after the load has been removed, as is often done in a firing test, may not be sufficient to assure good obturation for materials at low modulus. For these materials the total driving edge displacement while under load should be determined. The method described in this report, with certain modifications, could be adopted to measure the total displacement.

TABLE I  
 NYLON (ZYTEL 101) TEST RESULTS

Band No.	Force to Overcome Friction (lb)	Applied Torque (in - lb)	Band Pressure $P_b$ psi	$\mu$	$\sigma_{de}$ psi	$\delta_{de}$ (in.)
31		00			00	-.0006
32		00			00	+.0006
33		00			00	+.0004
19	860	1771	7636	.049	20,855	+.0009
20	930	1771	7908	.051	20,809	+.0011
21	900	1771	8726	.045	20,787	+.0012
5	1050	2214	7854	.058	26,971	+.0015
7	960	2156	7417	.056	25,280	+.0047
11	690	2214	7363	.041	25,708	+.0021
6	800	2666	6927	.050	30,928	+.0043
14	770	2666	7908	.042	30,894	+.0050
10	780	3318	8181	.041	36,028	+.0077
15	960	3118	8181	.051	36,225	+.0065
9	800	3378	8181	.043	39,043	+.0085
16	960	3378	7908	.053	39,219	+.0088

TABLE II  
 BOLTARON (6200) BAND TEST RESULTS

Band No.	Force to Overcome Friction (lb)	Applied Torque (in - lb)	Band Pressure $P_b$ psi	$\mu$	$\sigma_{de}$ psi	$\delta_{de}$ (in.)
1	780	0	4909	.069	0	-.0008
2	780	0	4254	.080	0	+.0008
3	780	0	4354	.083	0	-.0007
4	1075	1771	5454	.086	21,127	+.0014
5	1080	1771	4363	.108	21,175	+.0035
6	1165	1771	4909	.103	21,251	+.0032
7	1010	2214	4909	.089	26,117	+.0049
8	1145	2214	4909	.101	26,289	+.0077
9	780	2214	4909	.069	25,861	+.0061
10	875	2685	5181	.073	31,332	+.0089
11	875	2635	5454	.070	31,081	+.0100
12	1060	2685	5999	.077	31,244	+.0073
13	1300	3119	5454	.104	35,758	+.0121
14	1050	3119	4909	.093	36,171	+.0138
15	805	3119	4909	.071	36,210	+.0172

**BLANK PAGE**

APPENDIX A  
DETERMINATION OF COEFFICIENT OF FRICTION

The coefficient of friction,  $\mu$ , acting over the periphery of a rotating band can be expressed as a function of the radial band pressure,  $P_b$ , and the axial force,  $F_a$ , when the applied torque is zero. This is accomplished by solving the equations of equilibrium for  $\mu$ . The equations for equilibrium of forces and torques can be developed from a consideration of Figure 11.

$$\Sigma F_Z = 0$$

$$F_a = \sigma_{de} \ell N \left( \frac{D_g - D_\ell}{2} \right) (\tan \phi + \mu) + \mu P_b \pi \ell \left( \frac{D_g + D_\ell}{2} \right) \cos \phi. \quad (1)$$

$$\Sigma T_Z = 0$$

$$\begin{aligned} T_a = \sigma_{de} \ell N \left( \frac{D_g - D_\ell}{2} \right) \left( \frac{D_g + D_\ell}{4} \right) (1 - \mu \tan \phi) \\ - \mu P_b \pi \ell \left( \frac{D_g + D_\ell}{2} \right) \left( \frac{D_g + D_\ell}{4} \right) \sin \phi. \end{aligned} \quad (2)$$

$$\text{If } T_a = 0,$$

$$\sigma_{de} = \frac{\mu P_b \pi (D_g + D_\ell) \sin \phi}{N(D_g - D_\ell)(1 - \mu \tan \phi)}. \quad (2a)$$

Substituting Equation 2a into Equation 1,

$$F_a = + \frac{\mu P_b \pi (D_g + D_\ell) \ell}{2} \left( \cos \phi + \frac{\sin \phi \tan \phi + \mu \sin \phi}{1 - \mu \tan \phi} \right) \quad (3)$$

since  $\phi = 6^\circ$

$\sin \phi \tan \phi \ll \cos \phi$

$\therefore \sin \phi \tan \phi$  can be discarded.

$$\frac{2 F_a}{P_b \pi (D_g + D_\ell) \ell} = - \mu \left( \frac{\cos \phi - \mu \sin \phi + \mu \sin \phi}{1 - \mu \tan \phi} \right). \quad (4)$$

The right-hand side of Equation 4 can be expanded as an infinite series in  $\tan \phi$  and  $\mu$  as follows:

$$\frac{2 F_a}{P_b \pi (D_g + D_\ell) \ell} = -\mu \cos \phi (1 + \mu \tan \phi + \mu^2 \tan^2 \phi + \mu^3 \tan^3 \phi + \dots) \quad (5)$$

$$\tan \phi = \tan 6^\circ = .1051 = 1/9.5$$

$$\cos \phi = \cos 6^\circ = .9945 \approx 1$$

$$\frac{2 F_a}{P_b \pi (D_g + D_\ell) \ell} = \mu \left( 1 + \frac{\mu}{9.5} + \frac{\mu^2}{(9.5)^2} + \frac{\mu^3}{(9.5)^3} + \dots \right) \quad (6)$$

The above series in  $\mu$  converges for values of  $\mu < 9.5$ . That  $\mu$  must be less than 9.5 can be seen by considering the left side of the equation. If the left side is finite, as it is in this case, the series must converge. For the case where the series converges, a good approximation of  $\mu$  can be obtained by considering only a finite number of terms in the expansion. It can also be observed that when the higher order terms are neglected, the resulting value of  $\mu$  is higher than the true value. Therefore, if we neglect all but the first term as an initial approximation, the resulting value of  $\mu$  will be higher than the true value. If this resulting value of  $\mu$  is substituted back into Equation 6, the error involved by neglecting the higher order terms can be estimated.

## APPENDIX B

### ERROR ANALYSIS OF DRIVING EDGE PRESSURE

The driving edge pressure,  $\sigma_{de}$ , can be expressed as a function of the applied torque,  $T_a$ , the radial band pressure,  $P_b$ , the coefficient of friction,  $\mu$ , and certain geometric parameters by solving the torque equilibrium equation of the free body diagram shown in Figure 11. This functional relationship is expressed below:

$$\sigma_{de} = \frac{8 T_a + \mu P_b \pi \ell (D_g + D_\ell)^2 \sin \phi}{\ell N (D_g^2 - D_\ell^2) (1 - \mu \tan \phi)} \quad (1)$$

The magnitude of the terms,  $T_a$ ,  $P_b$ , and  $\mu$  appearing in Equation 1 are subject to certain inaccuracies. The cumulative effect of these inaccuracies on the magnitude of the  $\sigma_{de}$  will constitute an incremental error,  $d\sigma_{de}$ . This incremental error,  $d\sigma_{de}$ , can be expressed as a percent of  $\sigma_{de}$  by multiplying the ratio,  $d\sigma_{de}/\sigma_{de}$ , by 100

$$\text{percent error} = \frac{d\sigma_{de}}{\sigma_{de}} \times 100. \quad (2)$$

The incremental error,  $d\sigma_{de}$ , can be determined by differentiation.

$$d\sigma_{de} = \frac{\partial \sigma_{de}}{\partial T_a} dT_a + \frac{\partial \sigma_{de}}{\partial P_b} dP_b + \frac{\partial \sigma_{de}}{\partial \mu} d\mu \quad (3)$$

where

$$\frac{\partial \sigma_{de}}{\partial T_a} = \frac{8}{\ell N (D_g^2 - D_\ell^2) (1 - \mu \tan \phi)} \quad (4)$$

$$\frac{\partial \sigma_{de}}{\partial P_b} = \frac{\mu \pi (D_g + D_\ell)^2 \sin \phi}{N (D_g^2 - D_\ell^2) (1 - \mu \tan \phi)} \quad (5)$$

$$\frac{\partial \sigma_{de}}{\partial \mu} = \frac{1}{N(D_g^2 - D_\ell^2)(1 - \mu \tan \phi)} \times \left\{ \pi P_b (D_g^2 + D_\ell^2) \sin \phi + \frac{[8T_a + \mu \pi P_b \ell (D_g + D_\ell)^2 \sin \phi] \tan \phi}{\ell(1 - \mu \tan \phi)} \right\} \quad (6)$$

The above equations will be solved for a particular band, Boltaron Band No. 4 of this investigation.

$$\frac{\partial \sigma_{de}}{\partial T_a} = \frac{8}{.701} = 11.43 \frac{1}{\text{in.}^3} \quad (7)$$

$$\frac{\partial \sigma_{de}}{\partial P_b} = \frac{0.245}{1.403} = .175 \quad (8)$$

$$\frac{\partial \sigma_{de}}{\partial \mu} = 13,375 \text{ psi} \quad (9)$$

where  $\ell = 0.5 \text{ inch}$   
 $N = 12$   
 $D_g = 1.497 \text{ inch}$   
 $D_\ell = 1.457 \text{ inch}$   
 $\phi = 6^\circ$   
 $T_a = 1771 \pm 19.3 \text{ in} \cdot \text{lb}$   
 $P_b = 5454 \pm 272.7 \text{ psi}$   
 $\mu = 0.0856 \pm 0.01$

$$d\sigma_{de} = \frac{\partial \sigma_{de}}{\partial T_a} dT_a + \frac{\partial \sigma_{de}}{\partial P_b} dP_b + \frac{\partial \sigma_{de}}{\partial \mu} d\mu \quad (10)$$

$$d\sigma_{de} = 11.43 \times 19.3 + .175 \times 272.7 + 13,375 \times .01$$

$$= 221 + 47.7 + 133.8 = 402.5 \text{ psi}$$

$$\% \text{ Error} = 100X \frac{d\sigma_{de}}{\sigma_{de}} = \frac{402.5}{21,127} \times 100 = 1.9\%$$



## APPENDIX C

### DRIVING EDGE DISPLACEMENT

The total driving edge displacement of a rotating band, excluding that due to wear, consists of an elastic or recoverable displacement plus a plastic or permanent displacement. The elastic displacement for materials of high modulus, such as copper or iron, is generally small and can be disregarded without introducing any significant error in the total displacement. Thus, for example in a firing test, the measured displacement of the driving edge of the recovered bands does not include the elastic displacements which were recovered when the band left the tube.

The elastic displacement of the driving edge for materials of low modulus, such as plastics, may be quite large and should be considered in the total displacement. The total driving edge displacement can be expressed as a function of the normal stress,  $\sigma_x$ , on planes parallel to the driving edge; the yield stress of the material,  $\sigma_e$ ; the elastic and plastic modulus,  $E$  and  $E'$ ; and a length parameter for a band loaded as shown in Figure 14.

$$\frac{d\delta}{dX} = \epsilon \quad (1)$$

$$\epsilon_1 = \frac{\sigma_x}{E} \quad X > X_1 \quad (2)$$

$$\epsilon_2 = \frac{\sigma_e}{E} + \frac{\sigma_x - \sigma_e}{E'} \quad X > X_1 \quad (3)$$

$$\delta = \int_0^{X_1} \epsilon_2 dX + \int_{X_1}^{X_2} \epsilon_1 dX \quad (4)$$

Substitution of Equations 2 and 3 into Equation 4 yields:

$$\delta = \int_0^{X_1} \left( \frac{\sigma_e}{E} + \frac{\sigma_x - \sigma_e}{E'} \right) dX + \int_{X_1}^{X_2} \frac{\sigma_x}{E} dX \quad (5)$$

where  $\delta$  = driving edge displacement  
 $\sigma_x$  = normal stress on plane parallel to driving edge  
 $\sigma_e$  = yield stress of material  
 $E$  = modulus of elasticity  
 $E'$  = modulus of plasticity  
 $X_1$  = distance from driving edge over which normal stress exceeds yield stress  
 $X_2$  = width of land.

When the maximum normal stress,  $\sigma_{x_{\max}}$ , does not exceed the yield stress,  $\sigma_e$ , the first two integrals on the right side of Equation 5 are zero and the total displacement is elastic.

$$\delta = \int_0^{X_2} \frac{\sigma_x}{E} dX \quad \text{where } \sigma_x < \sigma_e. \quad (6)$$

For identical loading conditions (Figure 14), the stress distribution would be the same for all materials, provided the yield stress of the material is not exceeded. In that event, the elastic driving edge displacement,  $\delta$ , would vary inversely as the elastic modulus  $E$ . The elastic driving edge displacement of one material can then be expressed as a function of the elastic driving edge displacement of a second material.

$$\frac{\delta_1}{\delta_2} = \frac{E_2}{E_1}. \quad (7)$$

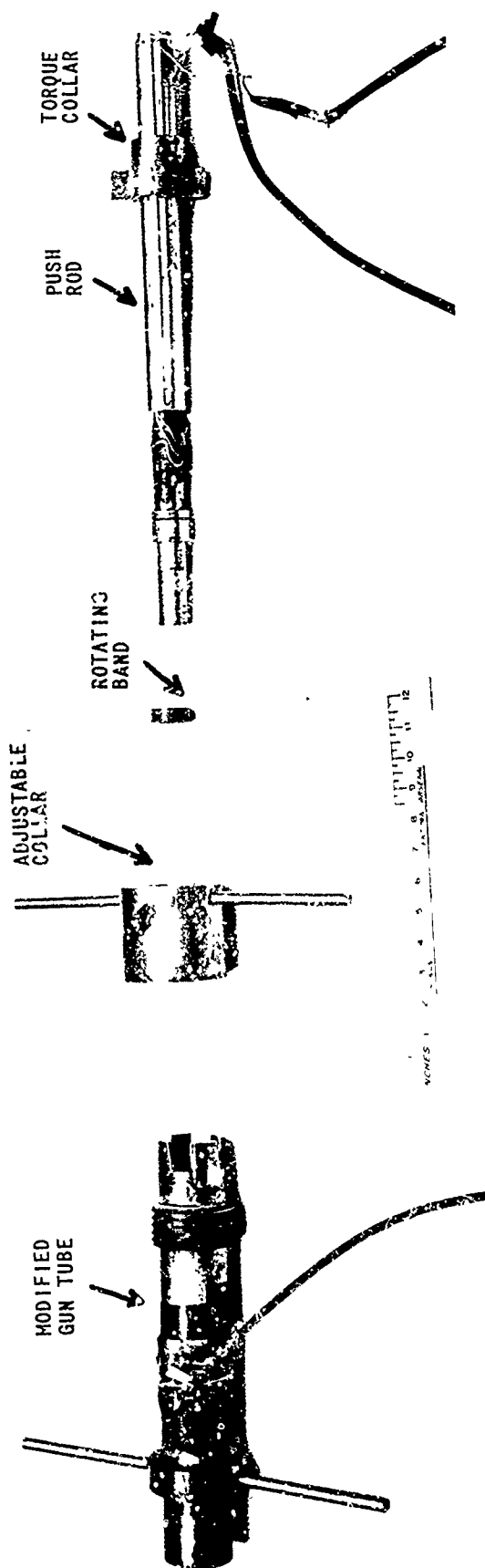
To illustrate the significance of this fact, the elastic driving edge displacement of nylon will be expressed as a function of the elastic driving edge displacement of copper:

$E_c$  = modulus of copper = 16,000,000 psi

$E_n$  = modulus of nylon = 230,000 psi

Then,  $\delta_{\text{nylon}} = 70 \delta_{\text{copper}}$ .

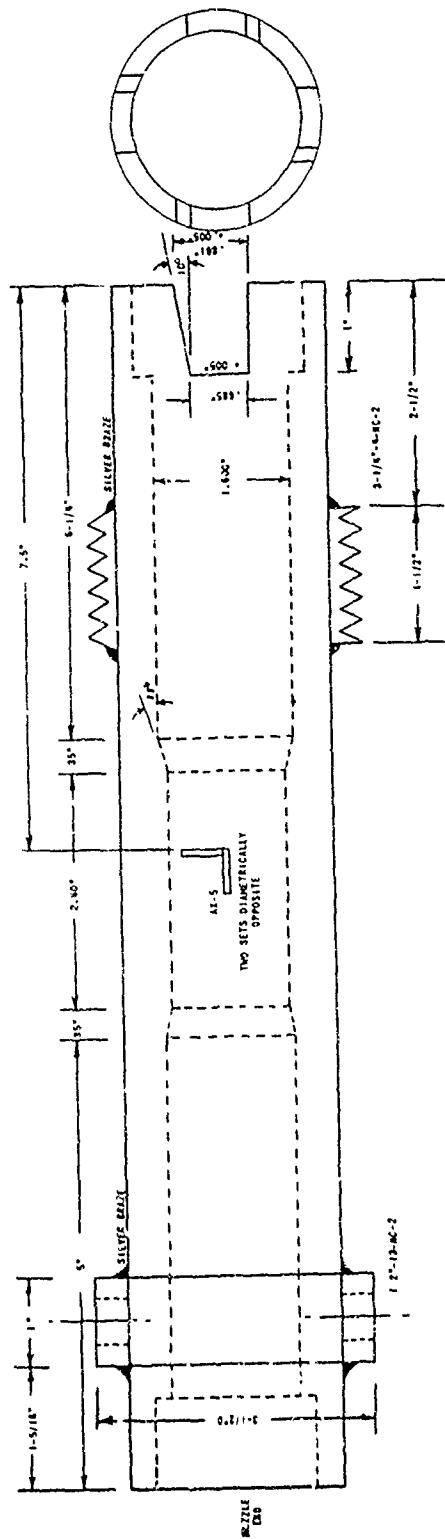
Thus, if the elastic driving edge displacement of copper were of the order of 0.0001 inch, the corresponding elastic driving edge displacement for nylon would be of the order of 0.007 inch.



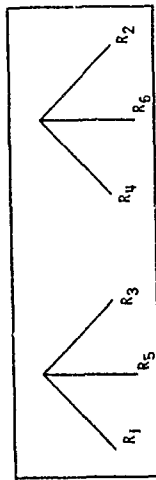
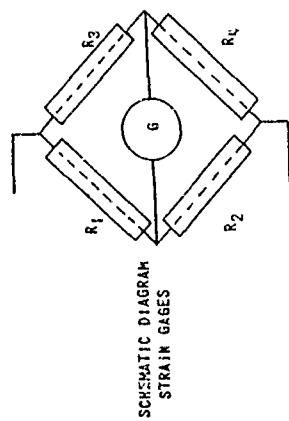
19-066-751/ORD-59

DISASSEMBLED TEST SETUP

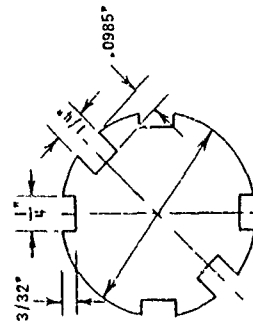
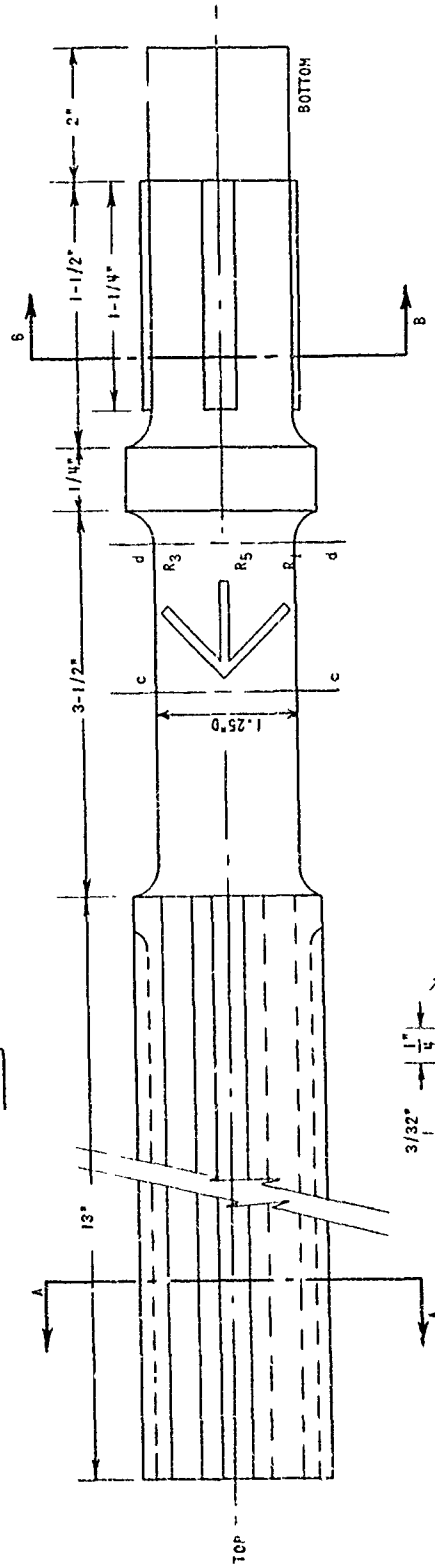
FIGURE 1



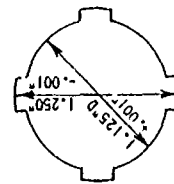
MODIFIED GUN TUBE



UNROLLED PERIPHERY BETWEEN PLANES c-c & d-d

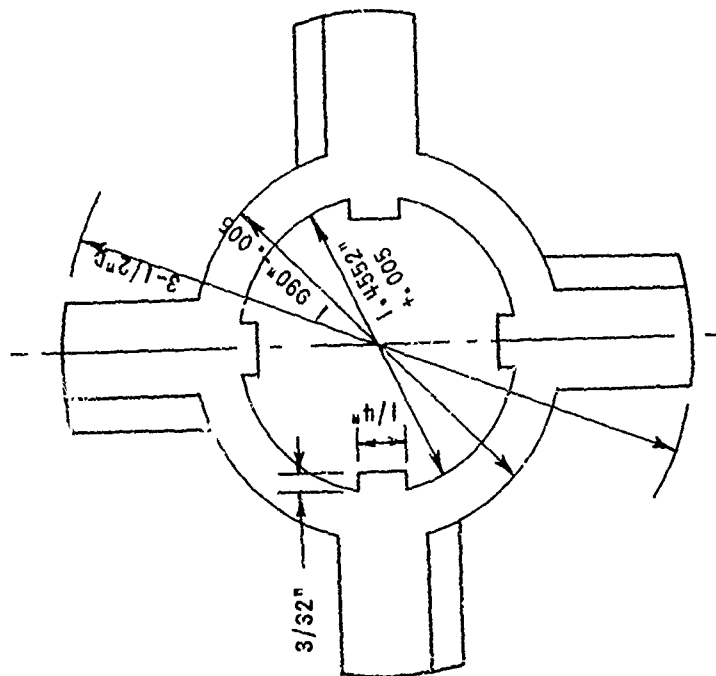


SECTION "A-A"

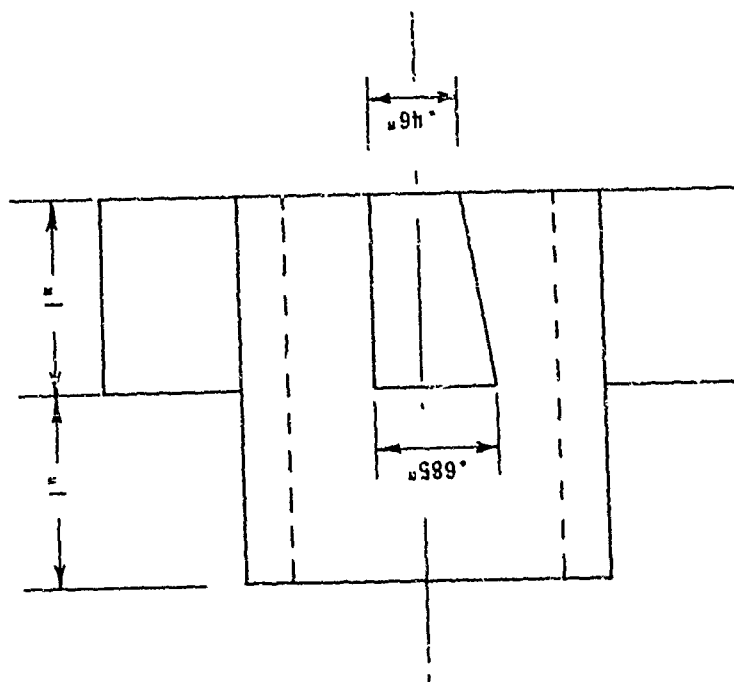


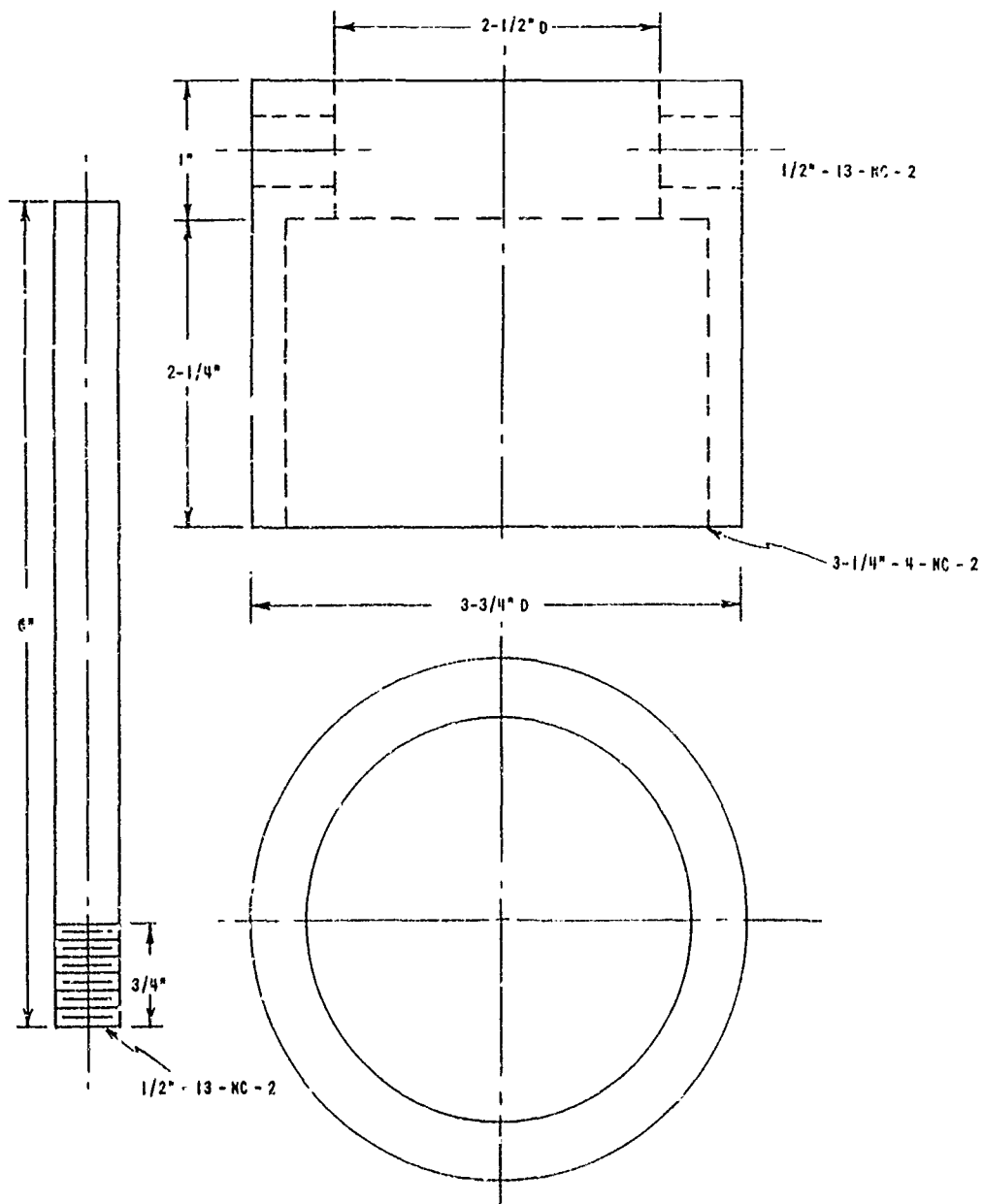
SECTION "B-B"

PUSH ROD

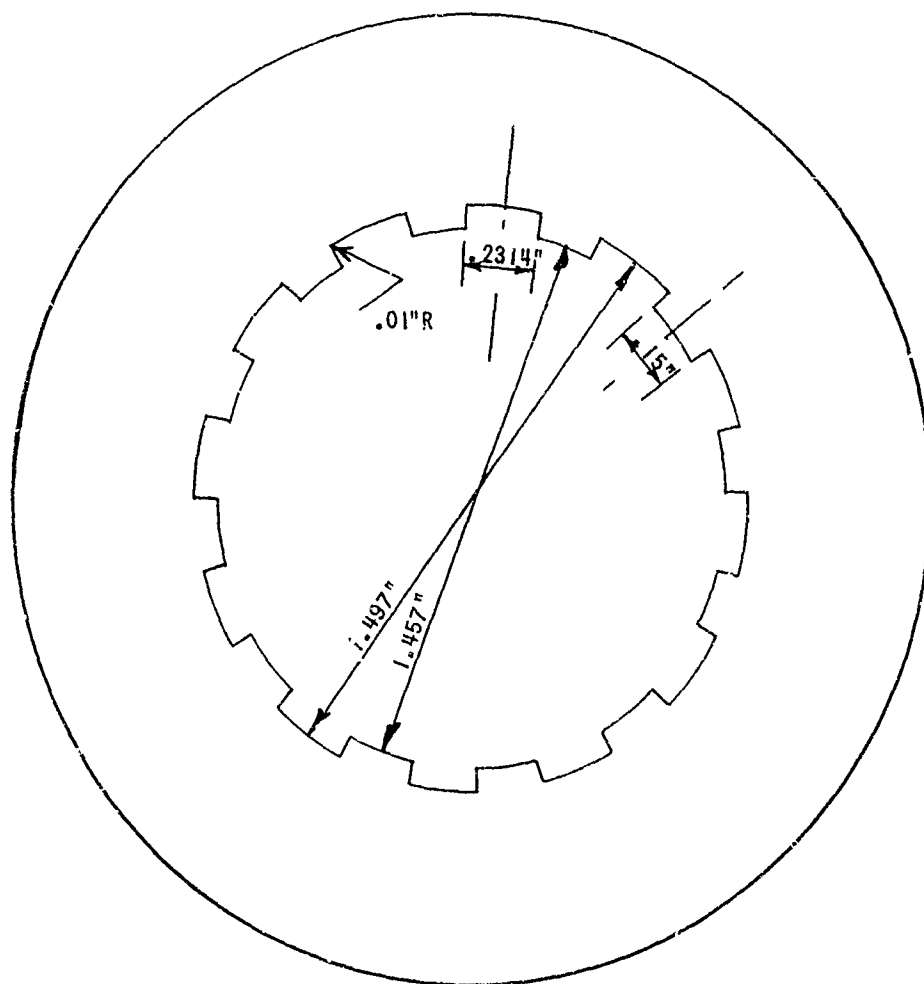


TORQUE COLLAR



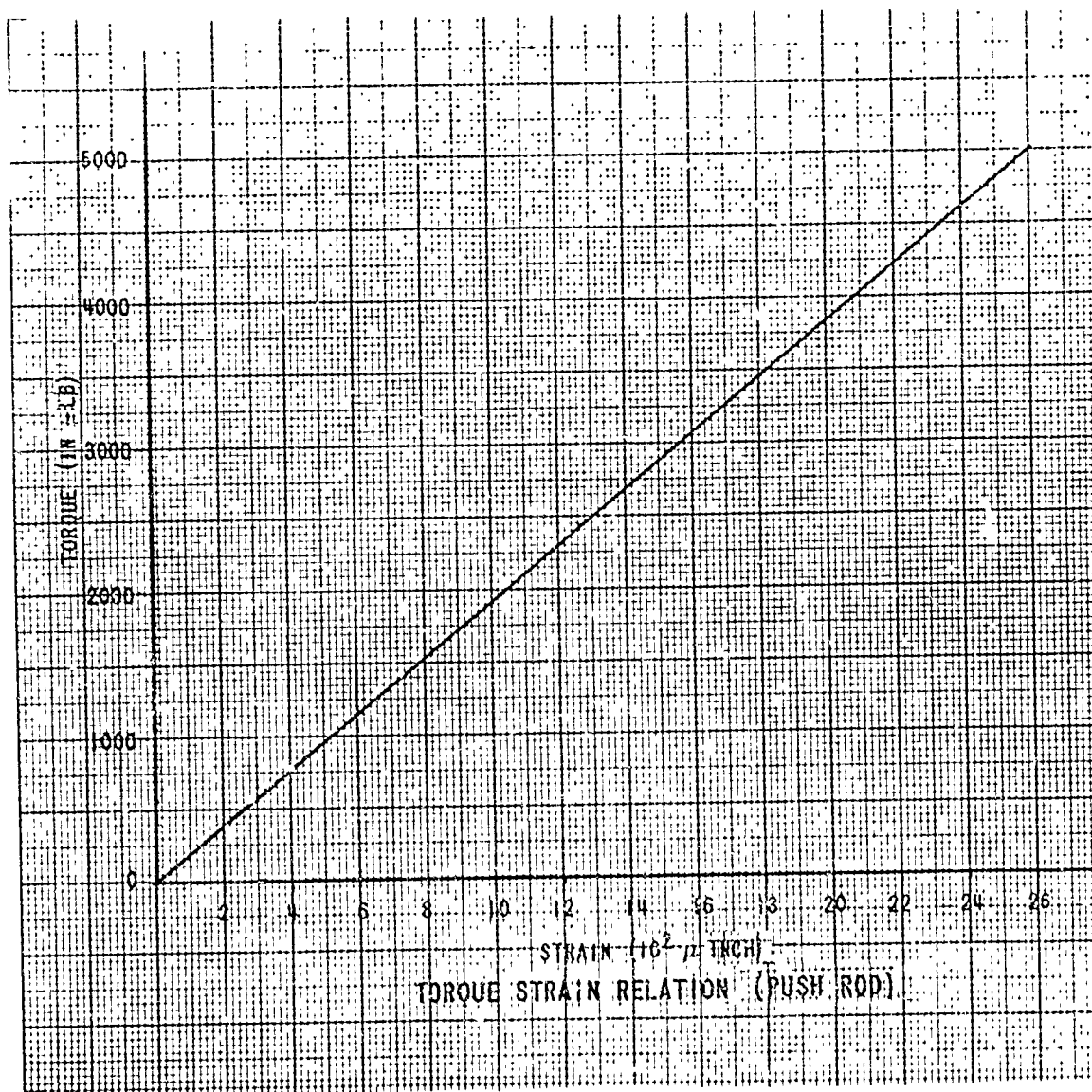


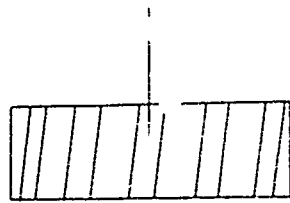
ADJUSTABLE COLLAR



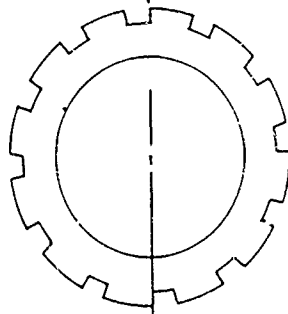
STANDARD 37MM RIFLING



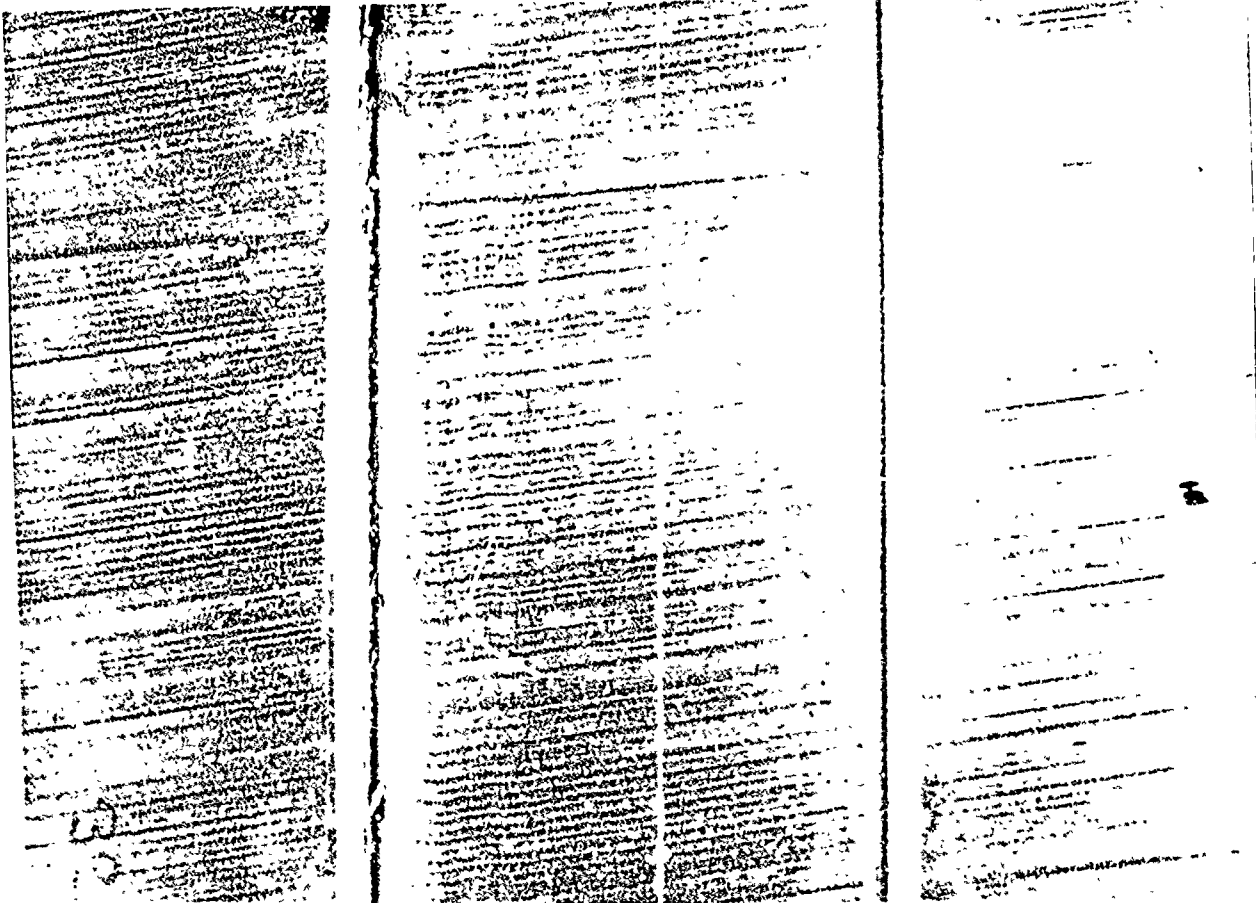




PHOTOMICROGRAPH SHOWS SURFACE  
PERPENDICULAR TO ARROW



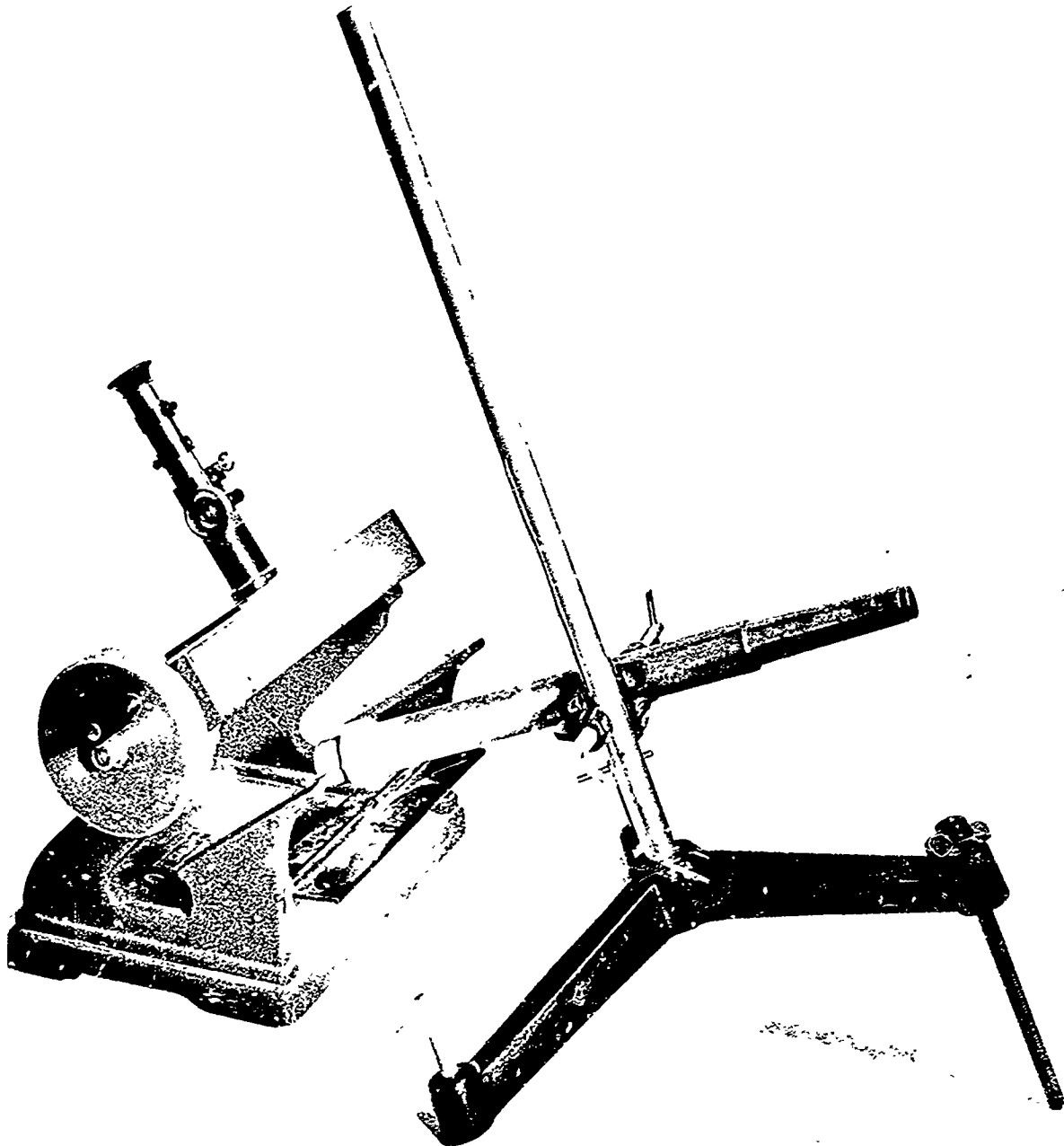
MEASURED GROOVE WIDTH



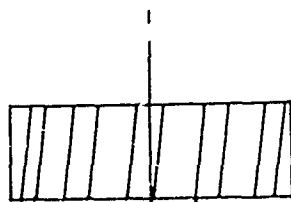
PHOTOMICROGRAPH OF BAND SURFACE

20X

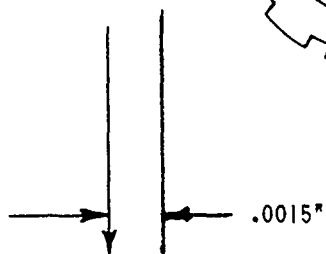
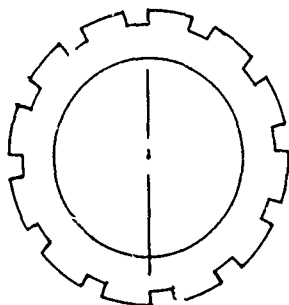
FIGURE 8



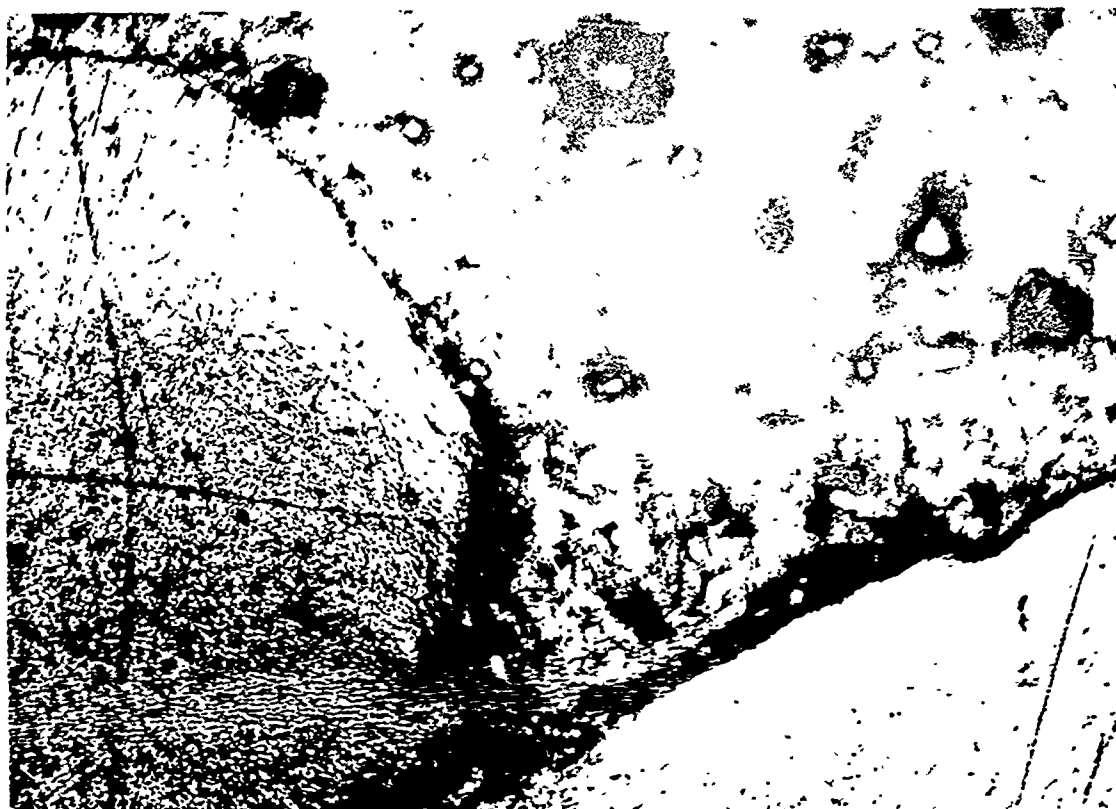
OPTICAL COMPARATOR AND BAND



PHOTOMICROGRAPH SHOWS SURFACE  
PERPENDICULAR TO ARROW

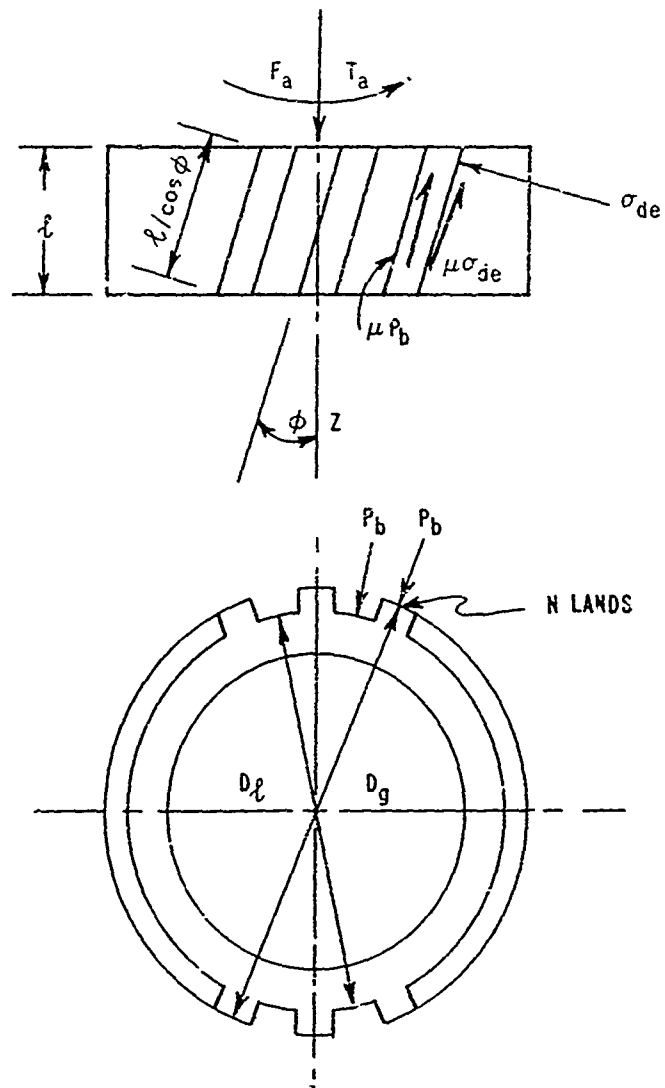


OUTER  
PERIPHERY

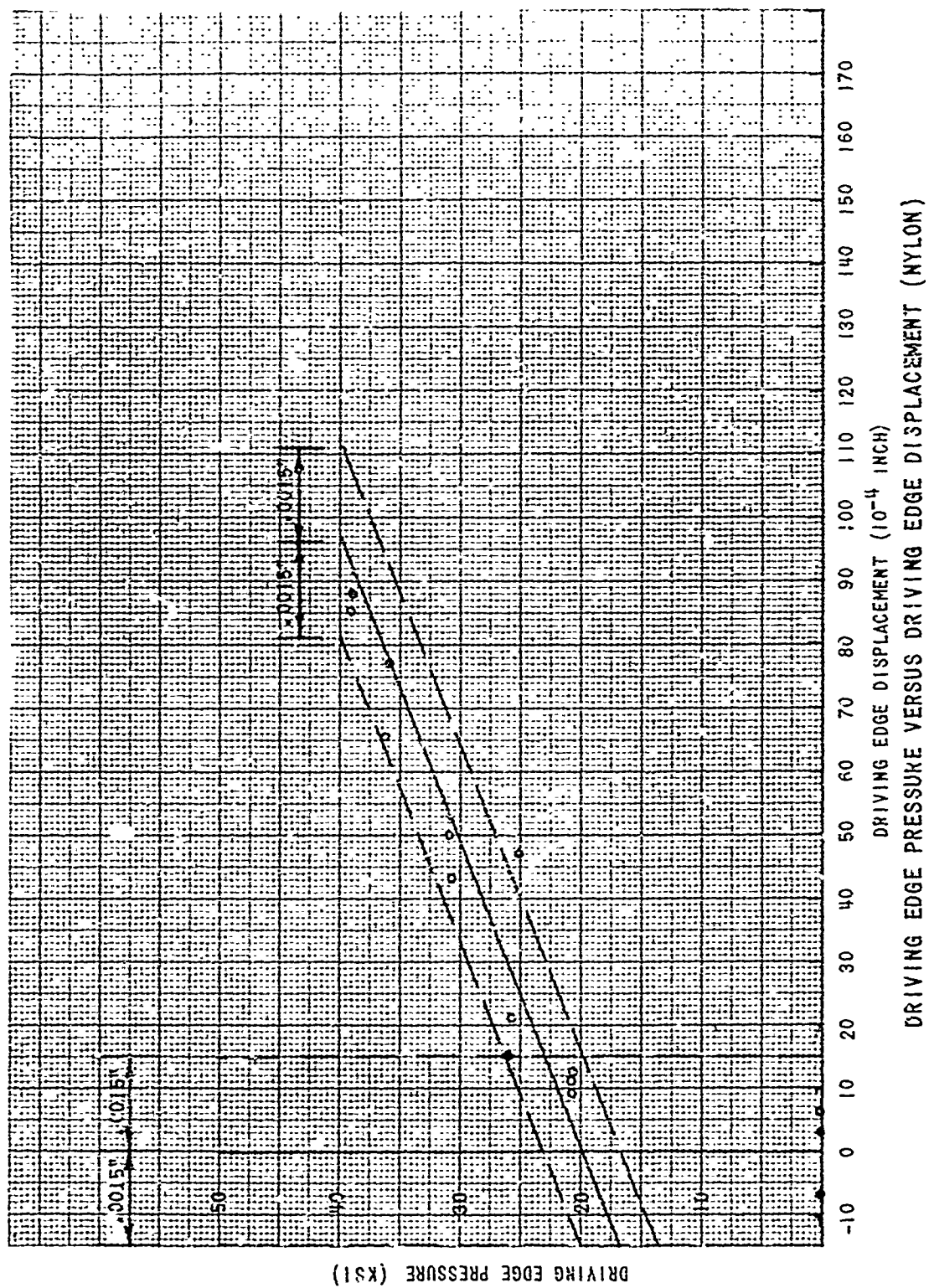


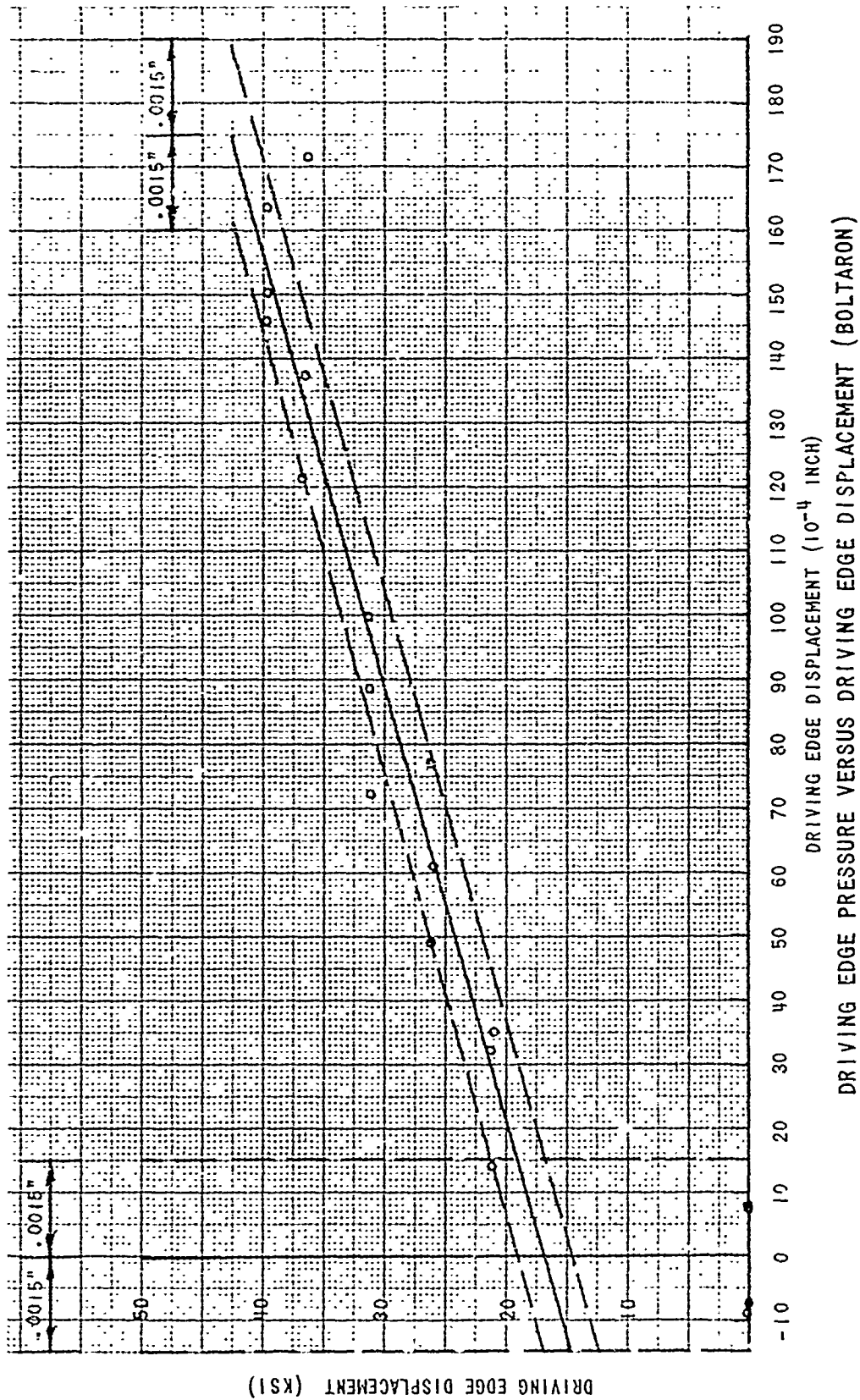
PHOTOMICROGRAPH OF GROOVE

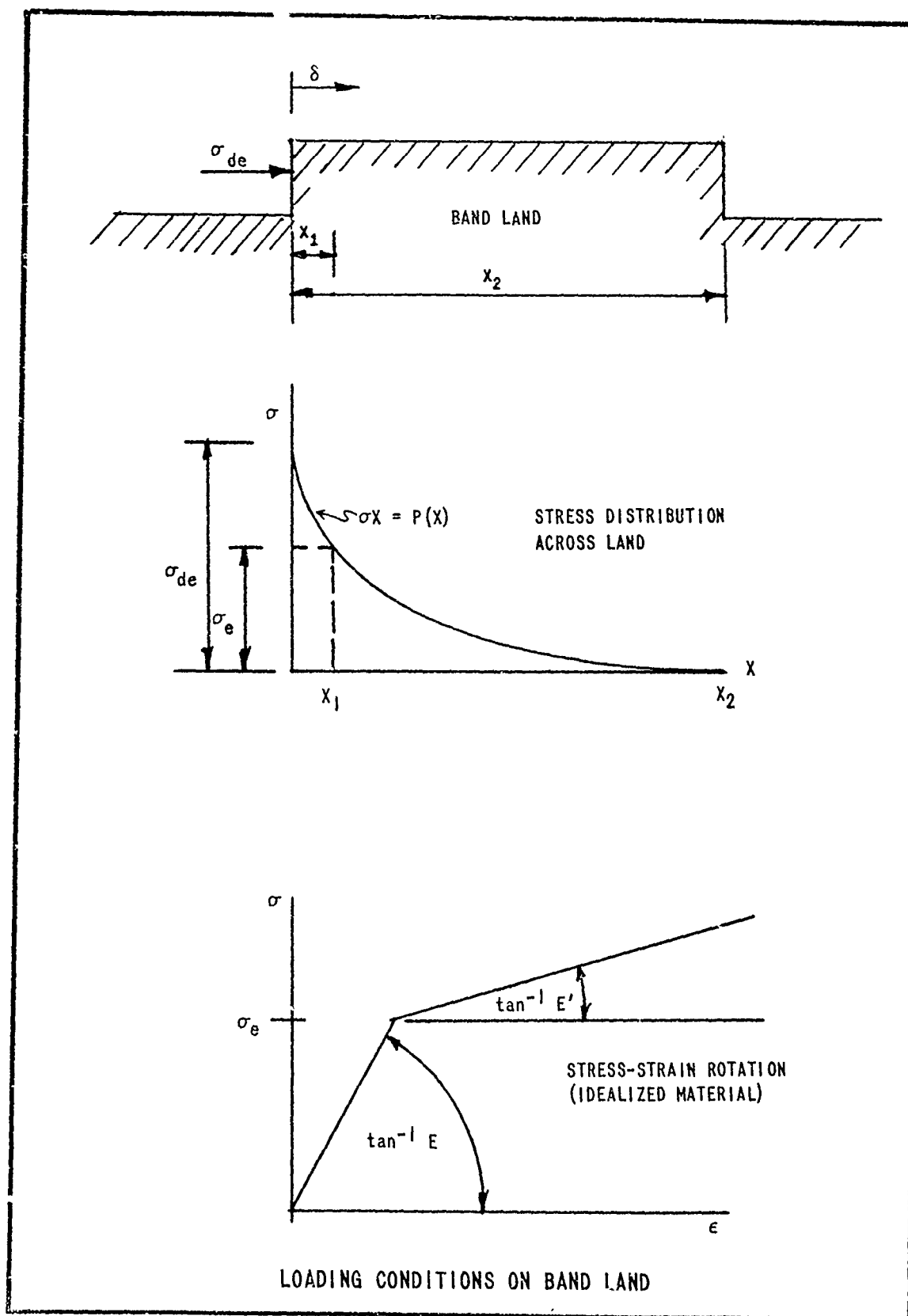
200X



FREE BODY DIAGRAM (ROTATING BAND)









AD Accession No.  
Watertown Arsenal Laboratories, Watertown 72, Mass.  
PLASTIC ROTATING BANDS: EVALUATION OF TWO PLASTICS -  
K. D. Robertson  
Report No. WAL TR 397.6/1, June 1960, 30 pp - tables -  
illus - appendices, OO Proj TW-120, DA Proj 5A04-03-  
005, Unclassified Report

A method is described to determine the maximum allowable driving edge pressure on rotating band materials. This method is then applied to determine the maximum allowable driving edge pressure for two plastic materials. An error analysis of the apparent driving edge pressure is included. Upper and lower limits on the experimentally determined maximum allowable driving edge pressure are given.

LIMITED DISTRIBUTION

UNCLASSIFIED  
1. Plastics  
2. Rotating band materials

I. Robertson,  
K. D.

II. OO Proj  
TW-120

III. DA Proj  
5A04-03-005

AD Accession No.  
Watertown Arsenal Laboratories, Watertown 72, Mass.  
PLASTIC ROTATING BANDS: EVALUATION OF TWO PLASTICS -  
K. D. Robertson  
Report No. WAL TR 397.6/1, June 1960, 30 pp - tables -  
illus - appendices, OO Proj TW-120, DA Proj 5A04-03-  
006, Unclassified Report

A method is described to determine the maximum allowable driving edge pressure on rotating band materials. This method is then applied to determine the maximum allowable driving edge pressure for two plastic materials. An error analysis of the apparent driving edge pressure is included. Upper and lower limits on the experimentally determined maximum allowable driving edge pressure are given.

LIMITED DISTRIBUTION

UNCLASSIFIED  
1. Plastics  
2. Rotating band materials

I. Robertson,  
K. D.  
II. OO Proj  
TW-120

III. DA Proj  
5A04-03-006

WATERTOWN ARSENAL  
TECHNICAL REPORT DISTRIBUTION

Report No.: WAL TR 397.6/1      Title: Plastic Rotating Bands: Evaluation  
of Two Plastics

To:	No. of Copies
Commanding Officer Watertown Arsenal Watertown 72, Mass. Attn: ORDBE-LXM, Tech. Info. Section	5
OMRO, Attn: RPD	1
Author	1
Office, Chief of Ordnance Department of the Army Washington 25, D. C. Attn: ORDIM - Ammunition Br.	1
ORDTB - Res. & Materials Br.	1
ORDTA - Ammunition Dev.	1
ORDTR - Weapons & Fire Control Br.	1
ORDTS - Infantry - Aircraft Weapons Systems	1
Commanding Officer Frankford Arsenal Bridge-Tacony Streets Philadelphia 37, Pa. Attn: ORDBA-1300	1
Commanding Officer Picatinny Arsenal Dover, New Jersey Attn: ORDBB-TE3	1
Tech. Library	1
Commanding Officer Watervliet Arsenal Watervliet, New York Attn: ORDBF-RT	2
Commanding General Aberdeen Proving Ground Aberdeen, Maryland Attn: Dev. & Proof Services	1
Ballistic Res. Lab.	1
Commandant, Ord. School	1

*Trans date: 6/15/60*

To:	No. of Copies
Commanding General Ordnance Weapons Command Rock Island, Illinois Attn: ORDOW-TX	1
Chief, Bureau of Ordnance Department of the Navy Washington 25, D. C. Attn: Rep-3	1
Commander Armed Services Tech. Info. Agency Arlington Hall Station Arlington 12, Virginia Attn: TIPDR	10
Commanding Officer Office of Ordnance Research Box CM, Duke Station Durham, North Carolina	1
Commander, Naval Ordnance Lab. Department of the Navy Silver Spring 19, Maryland Attn: Plastics Branch	1
Commander Naval Proving Ground Dahlgren, Virginia Attn: A&P Lab.	1
Commanding Officer Diamond Ordnance Fuze Labs. Washington 25, D. C. Attn: ORDTL 06.33 Tech. Ref. Section	1

TOTAL COPIES DISTRIBUTED -- 36

*Total number of copies printed - 45*  
*Copy for Publ Editor - 1*  
*Extra copies for author - 5*  
*Extra copies for Tech Info Sec 3*